

Methanol formation chemistry with revised reactions scheme

V. A. Sokolova^{1,2}

¹ Ural Federal University, 19 Mira street, Yekaterinburg, 620002, Russia; valeria.sokolova@urfu.ru

² Engineering Research Institute "Ventspils International Radio Astronomy Centre" of Ventspils University College, Inzenieru 101, Ventspils, LV-3601, Latvia

Received 20xx month day; accepted 20xx month day

Abstract The aim of the presented work is to analyze the impact of experimentally evaluated reactions of hydrogen abstraction on surfaces of interstellar grains on the chemical evolution of methanol and its precursors on grains and in the gas phase under conditions of cold dark cloud and during the collapse of the translucent cloud into the dark cloud. Analysis of simulation results shows that those reactions are highly efficient destruction channels for HCO and H₂CO on grain surfaces, and significantly impact the abundances of almost all molecules participating in the formation of CH₃OH. Next, in models with those reactions maximum abundances of methanol in gas and on grain surface decrease by more than 2-3 orders of magnitude in comparison to models without surface abstraction reactions of hydrogen. Finally, we study the impact of binding energies of CH₂OH and CH₃O radicals on methanol chemistry.

Key words: Astrochemistry – ISM: molecules – molecular processes – chemical networks – chemical modelling.

1 INTRODUCTION

Diverse molecular composition is one of the main properties of interstellar objects: it can include both simple and complex (more than 6 atoms) molecules (McGuire (2018)). Complex organic molecules (COMs, molecules containing more than 6 atoms, including C and H) are species of special interest, because they are actively involved in prebiotic chemistry and are associated with the origin of life (Herbst & van Dishoeck (2009)). Methanol (CH₃OH) is important molecule for the formation of more complex organic compounds according to a number of laboratory and theoretical studies (Öberg et al. (2009); Murga et al. (2020); Rivilla et al. (2019); Kochina et al. (2013)). It is assumed now (see e. g. Watanabe & Kouchi (2002); Fuchs et al. (2009); Linnartz et al. (2015)) that methanol in ISM forms on the surface of dust particles by hydrogenation of a carbon monoxide (CO) molecule, and then desorbs into the gas phase via thermal and non-thermal processes. Conventional hydrogenation that occurs on grain surfaces and leads from CO to CH₃OH (Tielens et al. (1991)) is as follows:



Recent laboratory experiments by Minissale et al. (2016) on atomic hydrogen exposure of carbon monoxide, formaldehyde, and methanol thin films on cold surfaces revealed an unexpected desorption phenomenon. The analysis of experiments led the authors to the conclusion that hydrogenation sequence of CO on grain surface must be expanded. It was shown that it is necessary to include additional

H₂-abstraction reactions (reverse reactions) for HCO and H₂CO into the scheme of surface methanol formation:



Given the fundamental importance of methanol for interstellar chemistry of complex organic molecules, we decided to study the impact of these reactions on chemical evolution under different conditions of interstellar medium. This paper is organized as follows. Section 2 is dedicated to utilized method of computation of molecular abundances and utilized physical models. Section 3 describes the modelling results. Discussion of obtained modelling results is presented in Section 4.

2 METHODS

2.1 Calculation molecular abundances

We use the MONACO code described in [Vasyunin et al. \(2017\)](#) to calculate abundances of species. It utilizes the rate equations method to numerically simulate the chemical evolution of the interstellar medium, and includes treatment of chemistry in the gas phase and on grain surfaces under non-stationary conditions. This code calculates time-dependent fractional abundances of species with respect to the total number of hydrogen nuclei for each species on a given time interval. In our study we run two types of models: with and without reverse reactions for HCO and H₂CO from [Minissale et al. \(2016\)](#), where the reaction (3) has the activation barrier $E = 202$ K ([Baulch et al. \(2005\)](#)).

In all models we use kinetic database utilized in [Vasyunin et al. \(2017\)](#), with binding energies $E_d(\text{CH}_2\text{OH}) = 5080$ K and $E_d(\text{CH}_3\text{O}) = 2540$ K (see Table 2 in [Wakelam et al. \(2017\)](#)). We denote the model without reverse reactions as Model I, and model with reverse reactions as Model II.

2.2 Utilized physical models

In our analysis we utilized two physical models. First model is a 0D model with time-dependent physical conditions that mimics the transition from a translucent cloud to a dark cloud. Second model represents typical static dark molecular cloud.

The model of collapse was taken from [Vasyunin & Herbst \(2013a\)](#) and consists of two stages. At the first "cold" stage the collapse proceeds in a free-fall regime and starts at a gas density $n_H = 3 \times 10^3$ cm⁻³ and visual extinction $A_V = 2^m$. The process continues until a density of 10^7 cm⁻³ is reached within 10^6 yrs of evolution. During the cold stage temperature linearly decreases from 20 to 10 K, and the gas temperature is assumed to be equal to the dust temperature. At the second "warm-up" stage temperature is growing from 10 to 200 K with a square-law over 2×10^5 years, that corresponds to models of the formation of intermediate-mass stars. Gas and dust temperatures are equal. Density and visual extinction remain constant. "High-metal" atomic initial composition corresponds to the values listed in column EA2 in Table 1 from [Wakelam & Herbst \(2008\)](#).

Model of a cold dark cloud corresponds to the model described in [Vasyunin & Herbst \(2013b\)](#) and represents a typical cold dark molecular cloud: $T = 10$ K, proton density $n_H = 10^5$ cm⁻³, visual extinction $A_V = 10^m$ and "low-metal" initial composition (see [Wakelam & Herbst \(2008\)](#), column EA1 in Table 1). Chemical evolution is simulated over a time span of 10^6 years.

3 RESULTS

The results of simulations are shown in Figures 1 — 3. Each plot represents time dependent abundances of methanol and some chemically related species.

3.1 Cold Cloud

In Figure 1 the abundances of methanol and chemically related species as a function of time in the gas phase and on the grain surface for the model of the cold dark cloud are presented.

In the Model II abundances of CH₃OH (both gaseous and on grain surface), gaseous CH₂OH, H₂CO, HCO and CO on grain surface show significant changes in comparison with the Model I.

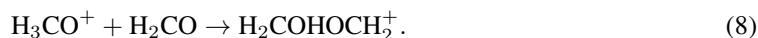
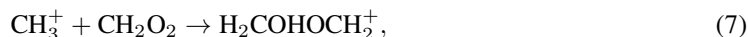
In the Model I, the main methanol formation routes are through the following reactions on the grain surface followed by the efficient reactive desorption (here and after in formulas and in figures all species on grain surface are marked with prefix 'g', species without 'g'-prefix are the gaseous species)



where the rate of the reaction (4) is higher by the factor of three than in reaction (5). In the Model II, reactions (4) and (5) become inefficient because of strong backward reactions in the nets of CH₃O and CH₂OH formation. Dissociative recombination of gaseous H₂COHOCH₂⁺ becomes the main route of gas phase methanol formation



Molecular ion H₂COHOCH₂⁺ in the Model II forms in reactions

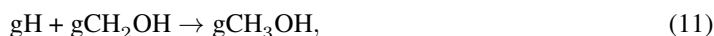


Analysis of chemical pathways shows that in both models the major reactions for CH₂OH and CH₃O formation on grain surface are



with equal rates. It means that smaller binding energy of CH₃O affects its abundance (it becomes higher) and helps CH₃O molecule to replace CH₂OH in reactions described above. At the same time, in the Model II the rate of reaction (3) is high enough to quickly destroy H₂CO. This is the reason of high HCO abundance on grain surface too. One should note that behaviour of HCO and CO maximum abundances on grain surface (see Figure (1)) are similar to each other and this can be also explained by high rate of reaction (3).

Methanol on grain surfaces in both models is mainly formed by reactions



In the Model II efficiencies of reactions (11) and (12) decreases and accretion of CH₃OH from gas becomes important in chemical evolution of methanol on grain surface.

Gaseous CH₂OH in the Model I can be formed only by reaction



The rate of this reaction in the Model II decreases by the factor of five and the main route of CH₂OH formation in gas is



Gaseous CH₃O in the Model I is formed in reactions



Reaction (16) becomes the most effective route of CH₃O formation and rate of reaction (15) drops down to zero in the Model II.

For CH₂OH and CH₃O, and then for CH₃OH, such changes in abundances and formation pathways can be explained by decreasing H₂CO abundance on grain surface as it was mentioned above.

3.2 Collapse from the translucent cloud into the dark cloud

3.2.1 Cold stage

Abundances of molecules in the gas and on grain surface for the first stage of the model of collapse are presented in Figure 2. Molecules with significant changes in abundances are the same as in the model of cold dark cloud.

In both types of models (Model I and II) gaseous methanol is formed in reactions (4), (5) and released in gas phase by thermal desorption from the grain surface. Rate of reaction (9) is higher by the factor of two than in the Model I. In the Model I, the main pathways of CH₃O and CH₂OH formation are reactions (9) and (10), but in the Model II almost all CH₃O molecules on grain surface are formed in the reaction



with temperatures of the medium of 18-20 K. At the same temperatures CH₂OH is formed in the reaction



Then during the collapse CH₃O begin to form in the reaction 10, and CH₂OH forms in reactions 9 and 18.

As it was described for the case of cold dark cloud, high rate of the reverse reaction (3) is responsible for decreasing of H₂CO abundance on grain surface and it affects on other reactions with this molecule.

3.2.2 Warm-up stage

Abundances of gaseous molecules and molecules on grains as a function of time for the second "warm" stage of the collapse are shown in Figure 3. Molecules with significant changes in abundances are the same as in the case of cold stage of the collapse. Warm-up stage is characterized by the square-law growing of temperature. Below we discuss molecular formation chains which occur at times when molecules start to approach their maximum values.

In both models (I and II) formation of CH₃O and CH₂OH becomes the object of our interest. Formation pathways of CH₃O (both gaseous and on the grain surface) are different from those described for the models of cold dark cloud and cold stage of the collapse. Gaseous CH₃O in both models (I and II) are produced effectively in reactions (16) and (15), but reaction (15) is less effective than reaction (16). In the Model I CH₃OH forms in reactions (4) and (5) with equal efficiencies, but in the model II CH₃OH forms in reaction (5) only. CH₂OH on grain surface in the model I forms in reaction (9), but in the Model II there is no efficient routes for its formation.

The main pathway of CH₃O formation on grains in both models is reaction (10) and the strongest reaction of its destruction is reaction (12). In the Model II reaction (10) becomes inefficient from chemical evolution of this molecule so CH₃O on the grain surfaces can be destructed only in reaction (12), and there is no routes for its formation. All changes in chemical evolution of gCH₃O can be explained by the influence of the added reverse reactions. In the Model II one can see that H₂CO on grain surfaces is destroyed in reaction (3) only, and there are no routes of effective CH₂OH, CH₃O formation on grain surfaces in contrast with Model I. This strongly affects on formation of CH₃OH, because CH₂OH on the grain surface is a key reactant in the reaction (5), and thus affects on formation of gaseous CH₃O through reaction (16). Moreover, rate of H₂CO destruction on grain surfaces in the Model II is higher by the factor of two than its formation and this directly affects on CH₃O formation in reaction (10) on grain surface.

In both models CH₂OH in gas and on grain surface is formed less effectively than CH₃O. Main formation pathways of gaseous CH₂OH are reaction (14) and less effective reaction (13). In the Model II reaction (13) inefficient in chemical evolution of gaseous CH₂OH, so only reaction (14) takes part in the formation of this molecule. Network analysis of CH₂OH formation on grain surfaces shows that in the Model I destruction of CH₂OH on grain surface in reaction (11) proceeds more effectively than its formation in reaction (9). In the Model II, reaction (9) disappears from chemical evolution, so

CH₂OH on grains can be destructed only in reaction (11). The most probable explanation is that CH₂OH chemical evolution is determined by faster destruction of H₂CO.

4 DISCUSSION AND CONCLUSIONS

In this study we analyzed the impact of added reverse reactions (reactions of H₂ abstraction) for HCO and H₂CO on the grain surfaces proposed by Minissale et al. (2016) on methanol chemistry. Analysis shows that the new reactions are highly efficient in the destruction of HCO and H₂CO and have a significant impact on abundances of molecules in the networks of methanol formation. In the models with reverse reactions abundances of CH₃OH in gas phase and on grain surface decreases by 2-3 orders of magnitude.

These results are in a somewhat mixed agreement with observations. In our model with added reverse reactions fractional abundances of methanol are about 10⁻¹¹ for the model of cold dark cloud and 10⁻¹⁰ and 10⁻⁶ for the first and the second stages of collapse correspondingly. Observed relative abundance of CH₃OH in cold dark medium is about 2 × 10⁻⁹ (Irvine et al. (1991); Agúndez & Wakelam (2013); Jiménez-Serra, et al. (2016); Vasyunina, et al. (2014)) and in hot cores - 10⁻⁷—10⁻⁵ (Bottinelli et al. (2007); Herbst & van Dishoeck (2009)). This discrepancy raises questions about the exact values of activation barriers of reverse reactions for HCO and H₂CO on grain surfaces, which will be solved in future studying.

Moreover, it is important to study CH₃O/CH₂OH evolution in methanol formation chain. In the recent research of Wakelam et al. (2017) binding energies for CH₂OH and CH₃O proposed to be E_d(CH₂OH) = E_d(CH₃O) = 4400 K. Figures 4, 5 and 6 show results of calculations for the model of cold dark cloud and for both stages of the collapse from translucent into dark cloud with E_d values from Wakelam et al. (2017). Here we will name these cases as Model Ia for model without reverse reactions and new E_d values, and Model IIa for model with reverse reactions and new E_d values. In case of the Model Ia, the most volatile molecules are CH₃O and CH₃OH. Such changes CH₃OH abundances probably can be explained by decreasing of reaction (4) rate.

In both stages of the collapse of translucent cloud into dark cloud the only molecules which abundances noticeably changed in both models (in comparison with Model I and II) are CH₂OH (both gaseous and on grains) and CH₃O in gas phase. Analysis of its formation pathways shows that changes in binding energies of CH₂OH and CH₃O affect only on efficiencies of reactions which were already described above. Therefore, the exact values of binding energies of CH₂OH and CH₃O does not affect on the way of methanol formation.

Acknowledgements The reported study was funded by RFBR according to the research project 18-32-00645. The author thanks A. B. Ostrovskii and A. I. Vasyunin for valuable discussions during the course of this work. The author thanks the anonymous referee for his helpful review of this paper.

References

- Agúndez M., Wakelam V., 2013, ChRv, 113, 8710 5
 Baulch, D. L., Bowman, C. T., Cobos, C. J., et al. 2005, Journal of Physical and Chemical Reference Data, 34, 757 2
 Bottinelli, S., Ceccarelli, C., Williams, J. P., et al. 2007, A&A, 463, 601 5
 Fillion, J.-H., Bertin, M., Danger, G., Duvernay, F., & Minissale, M. 2018, SF2A-2018: Proceedings of the Annual meeting of the French Society of Astronomy and Astrophysics, 15
 Fuchs, G. W., Cuppen, H. M., Ioppolo, S., et al. 2009, A&A, 505, 629 1
 Herbst, E., & van Dishoeck, E. F. 2009, ARA&A, 47, 427 1, 5
 Irvine, W. M., Oishi, M., & Kaifu, N. 1991, Icarus, 91, 2 5
 Jiménez-Serra I., et al., 2016, ApJL, 830, L6 5
 Kochina, O.V., Wiebe, D.S., Kalenskii, S.V., et al. 2013, Astron. Rep., 57 1
 Linnartz, H., Ioppolo, S., & Fedoseev, G. 2015, arXiv e-prints, arXiv:1507.02729 1

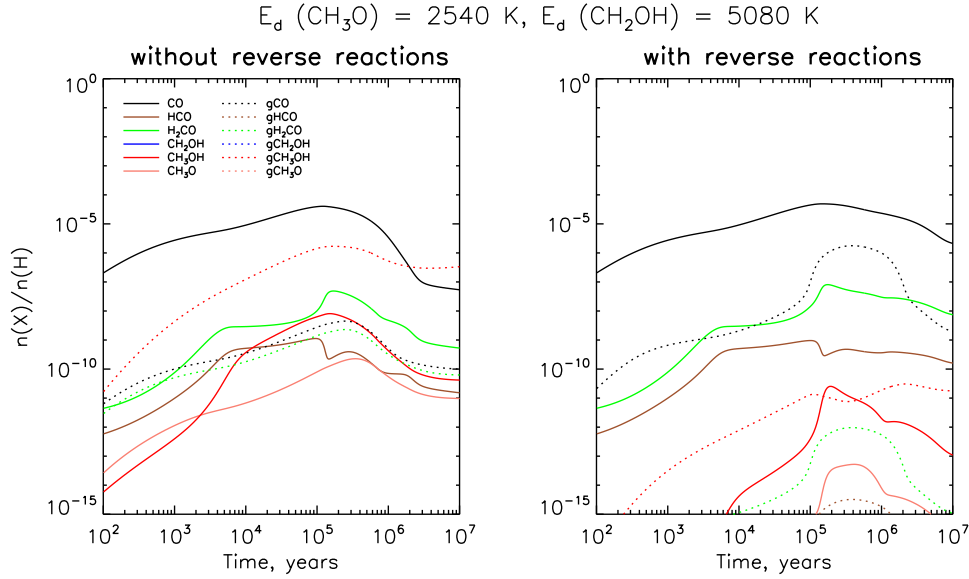


Fig. 1: Relative abundances of species versus time for the model of cold dark cloud. These plots correspond to calculations with $E_d(\text{CH}_2\text{OH}) = 5080 \text{ K}$ and $E_d(\text{CH}_3\text{O}) = 2540 \text{ K}$. Solid line represents molecules in gas phase, dashed line — molecules on grain surface. The evolution time range is 10^2 — 10^6 years.

McGuire, B. A. 2018, *ApJS*, 239, 17 [1](#)

Minissale, M., Moudens, A., Baouche, S., Chaabouni, H., & Dulieu, F. 2016, *MNRAS*, 458, 2953 [1](#), [2](#), [5](#)

Murga, M. S., Wiebe, D. S., Vasyunin, A. I., Varakin, V. N., Stolyarov, A. V. 2020, *Russian Chemical Reviews*, 89, 4 [1](#)

Öberg, K. I., Garrod, R. T., van Dishoeck, E. F., et al. 2009, *A&A*, 504, 891 [1](#)

Rivilla, V. M., Beltran, M. T., Vasyunin, A., et al. 2019, *MNRAS*, 483, 1 [1](#)

Tielens, A. G. G. M., Tokunaga, A. T., Geballe, T. R., et al. 1991, *ApJ*, 381, 181 [1](#)

Vasyunin, A. I., Caselli, P., Dulieu, F., & Jiménez-Serra, I. 2017, *ApJ*, 842, 33 [2](#)

Vasyunin, A. I., & Herbst, E. 2013, *ApJ*, 769, 34 [2](#)

Vasyunin, A. I., & Herbst, E. 2013, *ApJ*, 762, 86 [2](#)

Vasyunina T., et al., 2014, *ApJ*, 780, 85 [5](#)

Wakelam, V., Loison, J.-C., Mereau, R., & Ruaud, M. 2017, *Molecular Astrophysics*, 6, 22 [2](#), [5](#)

Wakelam, V., & Herbst, E. 2008, *ApJ*, 680, 371 [2](#)

Watanabe, N., & Kouchi, A. 2002, *ApJ*, 571, L173 [1](#)

$$E_d(\text{CH}_3\text{O}) = 2540 \text{ K}, E_d(\text{CH}_2\text{OH}) = 5080 \text{ K}$$

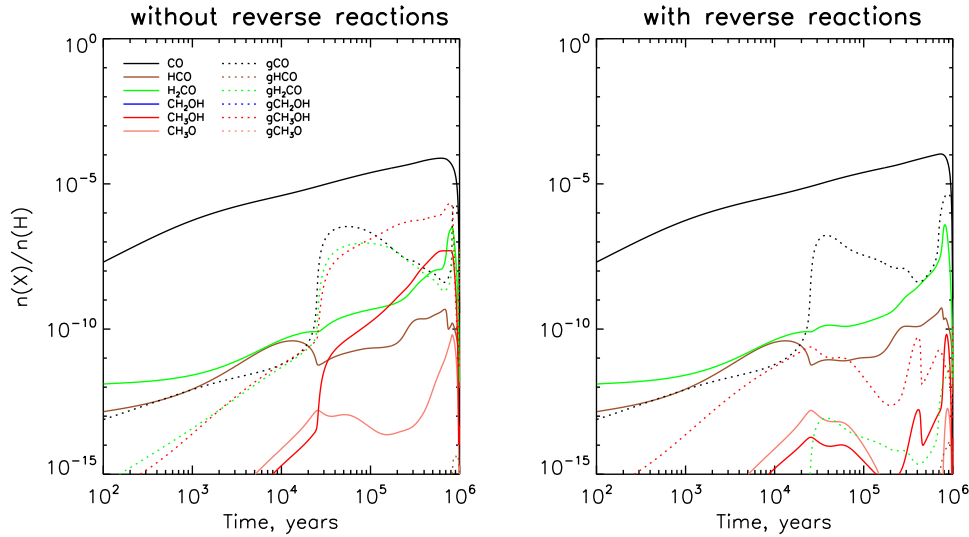


Fig. 2: Relative abundances of species versus time for the "cold" stage of the collapse model. These plots correspond to calculations with $E_d(\text{CH}_2\text{OH}) = 5080 \text{ K}$ and $E_d(\text{CH}_3\text{O}) = 2540 \text{ K}$. Solid line represents molecules in gas phase, dashed line — molecules on grain surface. The evolution time range is 10^2 — 10^6 years.

$$E_d(\text{CH}_3\text{O}) = 2540 \text{ K}, E_d(\text{CH}_2\text{OH}) = 5080 \text{ K}$$

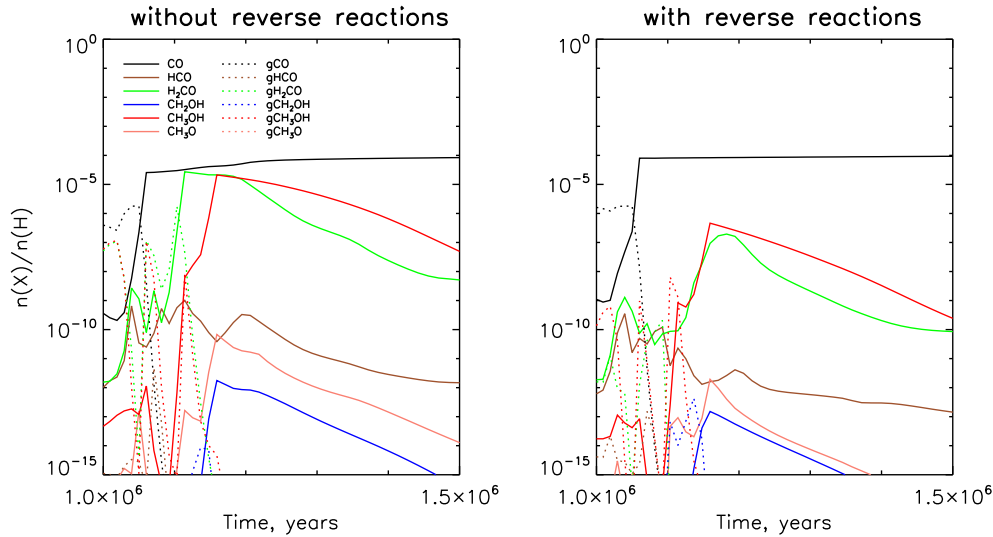


Fig. 3: Relative abundances of species versus time for the "warm-up" stage of the collapse model. These plots correspond to calculations with $E_d(\text{CH}_2\text{OH}) = 5080 \text{ K}$ and $E_d(\text{CH}_3\text{O}) = 2540 \text{ K}$. Solid line represents molecules in gas phase, dashed line — molecules on grain surface. The evolution time range is 1 — 1.5×10^6 years.

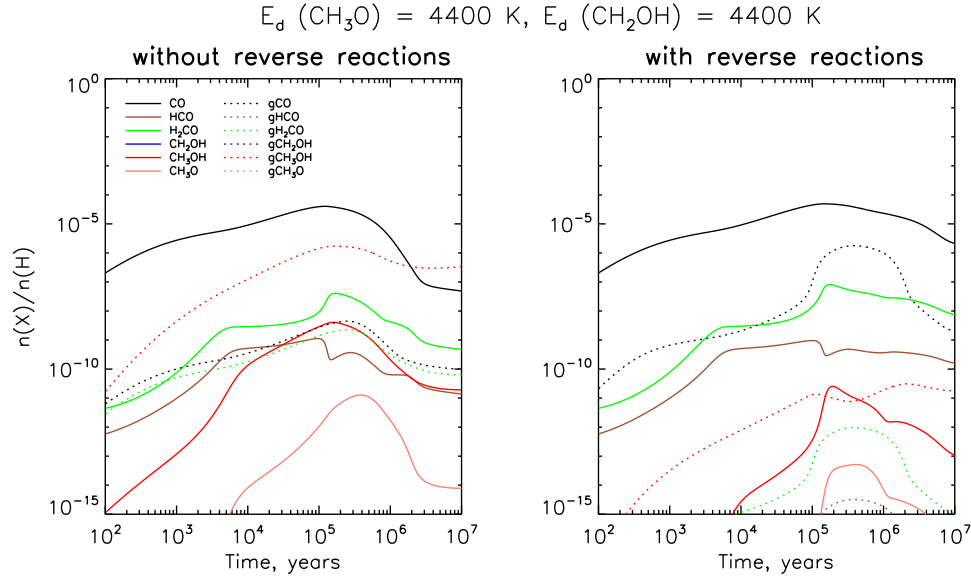


Fig. 4: Relative abundances of species versus time for the model of cold dark cloud. These plots correspond to calculations with $E_d(\text{CH}_2\text{OH}) = E_d(\text{CH}_3\text{O}) = 4400 \text{ K}$. Solid line represents molecules in gas phase, dashed line — molecules on grain surface. The evolution time range is 10^2 — 10^6 years.

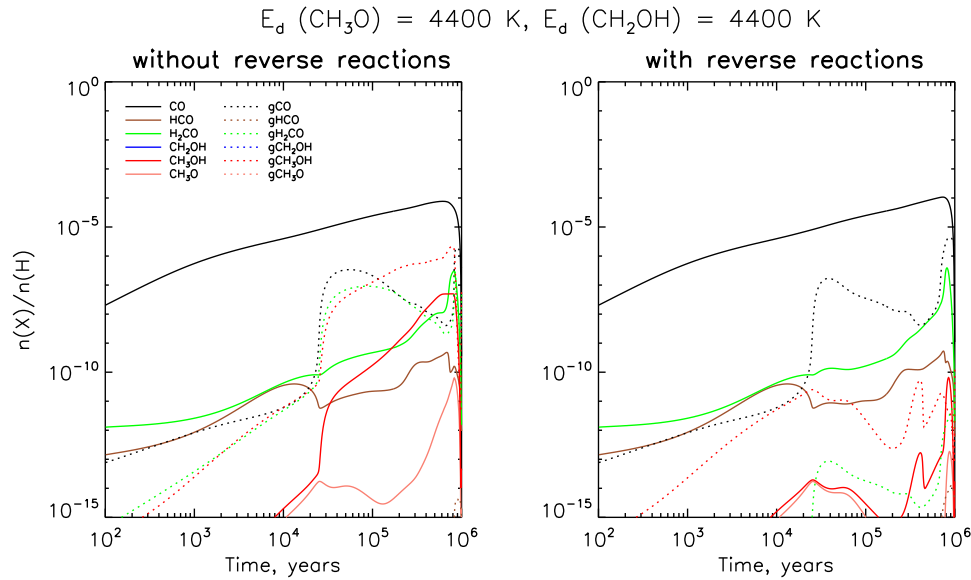


Fig. 5: Relative abundances of species versus time for the "cold" stage of the collapse model. These plots correspond to calculations with $E_d(\text{CH}_2\text{OH}) = E_d(\text{CH}_3\text{O}) = 4400 \text{ K}$. Solid line represents molecules in gas phase, dashed line — molecules on grain surface. The evolution time range is 10^2 — 10^6 years.

$$E_d(\text{CH}_3\text{O}) = 4400 \text{ K}, E_d(\text{CH}_2\text{OH}) = 4400 \text{ K}$$

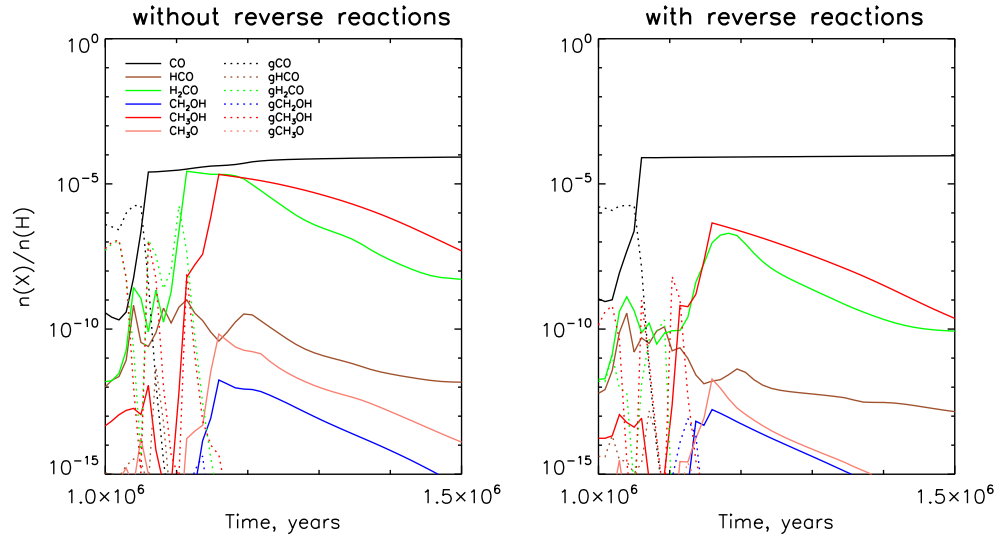


Fig. 6: Relative abundances of species versus time for the "warm-up" stage of the collapse model. These plots correspond to calculations with $E_d(\text{CH}_2\text{OH}) = E_d(\text{CH}_3\text{O}) = 4400 \text{ K}$. Solid line represents molecules in gas phase, dashed line — molecules on grain surface. The evolution time range is $1-1.5 \times 10^6$ years.